Independent vasomotor control of rat tail and proximal hairy skin

Mutsumi Tanaka[1], Youichirou Ootsuka[2], Michael J. McKinley[1] and Robin M. McAllen[1]

[1]*Howard Florey Institute of Experimental Physiology and Medicine, University of Melbourne, Parkville, Victoria 3010, Australia*
[2]*Department Human Physiology, School of Medicine, Flinders University, Bedford Park, South Australia 5042, Australia*

Quantitative differences are known to exist between the vasomotor control of hairy and hairless skin, but it is unknown whether they are regulated by common central mechanisms. We made simultaneous recordings from sympathetic cutaneous vasoconstrictor (CVC-type) fibres supplying back skin (hairy) and tail (hairless) in urethane-anaesthetized, artificially ventilated rats. The animal's trunk was shaved and encased in a water-perfused jacket. Both tail and back skin CVC-type fibres were activated by cooling the trunk skin, and independently by the resultant fall in core (rectal) temperature, but their thresholds for activation differed (skin temperatures 38.8 ± 0.4°C *versus* 36.8 ± 0.4°C, core temperatures 38.1 ± 0.2°C *versus* 36.8 ± 0.2°C, respectively; $P < 0.01$). Back skin CVC-type fibres were more responsive to skin than to core cooling, while the reverse applied to tail fibres. Back skin CVC-type fibres were less responsive than tail fibres to prostaglandin E_2 (PGE_2) microinjected into the preoptic area. Spectral analysis showed no significant coherence between tail and back skin CVC-type fibre activities during cooling. After preoptic PGE_2 injection, a coherent peak at 1 Hz appeared in some animals; this disappeared after partialization with respect to ventilatory pressure, indicating that it was attributable to common ventilatory modulation. Neuronal inhibition in the rostral medullary raphé by microinjected muscimol (2 mM, 60–120 nl) suppressed both tail and back skin CVC-type fibre activities, and prevented their responses to subsequent skin cooling. These results indicate that thermoregulatory responses of hairless and hairy skin vessels are controlled by independent neural pathways, although both depend on synaptic relays in the medullary raphé.

(Received 27 February 2007; accepted after revision 11 April 2007; first published online 12 April 2007)
Corresponding author R. M. McAllen: Howard Florey Institute of Experimental Physiology and Medicine, University of Melbourne, Parkville, Victoria 3010, Australia. Email: rmca@florey.edu.au

Thermoregulation depends partly upon controlling the circulation to periphery, to increase or decrease heat dissipation to the environment. The rat's tail, in particular, is a major organ for thermoregulation, and its circulation is regulated by sympathetic vasoconstrictor nerves under the control of the brain. Central temperature receptors, principally in the preoptic area, regulate the activity of the sympathetic vasoconstrictor nerves to the tail (Zhang *et al.* 1997; Owens *et al.* 2002; Tanaka *et al.* 2002); cutaneous temperature receptors also influence this outflow in a homeostatic manner (Owens *et al.* 2002; Ootsuka *et al.* 2004; Ootsuka & McAllen, 2006).

The rat's tail is not its only site for non-evaporative heat loss, however. Other hairless skin areas such as the plantar surface of the paw are also important for thermoregulation, and the blood flow to these areas also increases substantially with whole body heating (Key & Wigfield, 1994) and with preoptic warming (Zhang *et al.* 1995). In line with this common function, cutaneous vasoconstrictor fibres supplying the rat's tail and foot show common rhythmic discharge patterns, indicating that the central neural mechanisms which control them may be substantially the same (Smith & Gilbey, 2000).

In contrast, fur covered areas of skin are thought to be less important for thermoregulatory function (Key & Wigfield, 1994), and blood flow to these regions increases only modestly during heat exposure (Rendell *et al.* 1998). Another regional difference in cutaneous vasomotor control has been noted in the case of conditioned fear, during which there is cutaneous vasoconstriction in the tail and paw but not over the head and back (Vianna & Carrive, 2005). Although it has been suggested that the cutaneous vasoconstrictor fibres supplying hairy skin differ functionally from those of hairless skin (Jänig & Häbler, 2003), no study has yet directly compared their thermoregulatory

 DOI: 10.1113/jphysiol.2007.131292

properties. It is unclear whether such differences in control are qualitative or merely quantitative. Nor is it clear whether they are regulated by the same central neural pathways.

The present study directly compares the thermoregulatory behaviour and activity patterns of the cutaneous vasomotor supply to hairy skin with that to the rat's tail, by making simultaneous recordings from identified sympathetic fibres in anaesthetized rats. The study also includes comparison of their responses to experimental fever induced by prostaglandin E_2 microinjection into the preoptic area, and tests whether their central control pathways both involve a critical synaptic relay in the medullary raphé (Rathner & McAllen, 1999; Tanaka *et al.* 2002; Ootsuka *et al.* 2004).

Methods

Seventeen adult male Sprague–Dawley rats (290–510 g) were used in this study (8 for preliminary experiments and 9 for the main series). All experiments were carried out in accordance with guidelines of the National Health and Medical Research Council of Australia and were approved by the Animal Experimentation Ethics Committee of the Howard Florey Institute.

Animals were anaesthetized initially with pentobarbitone sodium (30–50 mg kg^{-1}, I.P.) and the hair over the trunk was shaved. The trachea was cannulated and animals were then artificially ventilated with 2% isofluorane (Forthane; Abbott Australia Pty Ltd, NSW, Australia) in pure oxygen. Respiratory pressure was monitored via a pressure transducer attached to a side tube and expired CO_2 concentration was monitored by a CO_2 analyser (ADC, Hoddesdon, Herts, UK). Ventilation was adjusted to keep expired CO_2 between 3.5 and 4.5%. The right femoral artery and vein were cannulated for monitoring blood pressure and intravenous administration of drugs, respectively. A water-perfused silastic jacket was positioned around the animal's shaved trunk, and the temperature of the perfusion water was used to manipulate skin and body temperature. Skin temperature was measured as the average of three thermocouples placed across the trunk between the skin and water jacket. Core temperature was measured by a thermocouple inserted 5 cm into the rectum. Core temperature was maintained between approximately 37 and 38°C by perfusion of the jacket at 150–180 ml min^{-1} with water from a reservoir maintained at 43–45°C. Cooling was achieved by switching the perfusion pump input to cold water (Owens *et al.* 2002).

The animal was then mounted prone in a stereotaxic apparatus according to the coordinate system of Paxinos & Watson (1998), and burr holes were made in the skull over the rostral hypothalamus and the medial medulla. The tail and the upper back were dissected to expose sympathetic nerves to the tail and the back skin, as detailed below. When surgery was complete, isofluorane was gradually withdrawn and replaced by urethane (1.0–1.2 g kg^{-1}, I.V.). The depth of anaesthesia was frequently assessed throughout the experiment by testing withdrawal and corneal reflexes, and small additional doses of urethane (25–50 mg, I.V.) were administered if necessary to abolish those reflexes.

Sympathetic nerve fibre recording

In eight rats (preliminary experiments), whole nerve recordings were made of the nerve supply to the back skin. In nine other rats (main series), the nerves to the back skin were split to record few-fibre activity, and simultaneous recordings were made from postganglionic sympathetic fibres in the lateral collector nerve of the tail (tail sympathetic nerve activity: tail SNA), as described elsewhere (Owens *et al.* 2002). A pool filled with liquid paraffin was constructed around the tail. Connective tissue was removed from the nerve trunk, which was cut distally and desheathed. The central end of the nerve filament was placed over a silver-wire hook electrode, and its efferent activity was recorded differentially with respect to a nearby thread of connective tissue, amplified (10 000-fold) and filtered (60–500 Hz).

The nerve supplying back skin at the lower thoracic level on the animal's right side was identified as it entered the subcutaneous tissue and dissected free from subcutaneous tissue and fat. The connective tissue sheath was removed from the nerve trunk and the nerve was cut distally. Under a paraffin pool, paired silver wire electrodes were used to make differential recordings of efferent activity in the central end of the nerve with respect to a thread of connective tissue placed over the reference electrode. In preliminary experiments, whole efferent nerve activity was recorded; in subsequent experiments, efferent filaments were split from the nerve. Back skin SNA was amplified (10 000-fold) and filtered (40–800 Hz for whole nerve activity, 50–700 Hz for filaments).

Both tail and back skin SNA spikes were displayed continuously on an oscilloscope. Spikes that passed a selected threshold voltage were discriminated and counted in 10 s bins using a computer-based recording and analysis system (CED POWER1401 and Spike 2 software; CED, Cambridge, UK). Raw signals for both tail and back skin SNA were sampled at 5000 Hz and recorded for subsequent spike separation off-line (using Spike2). Blood pressure (digitized at 100 Hz) and respiratory pressure (digitized at 10 Hz) were also recorded with Spike 2. Heart rate was computed from the blood pressure signal.

At the end of the experiment, hexamethonium chloride (Sigma; 50 mg kg^{-1} in saline) was given intravenously

to confirm that the recorded efferent nerve activity was postganglionic sympathetic.

Experimental procedures and analysis

Responses to skin and core cooling. Tail SNA and back skin SNA were first tested for thermosensitivity by their excitatory response to passing cold water through the water jacket (see Results).

Response to PGE_2 injection into the preoptic area. Prostaglandin E_2 (PGE_2; MP Biomedicals) was initially dissolved in pure ethanol and then diluted with artificial cerebrospinal fluid (aCSF), such that the final concentrations of PGE_2 and ethanol were 25 ng $(100\ nl)^{-1}$ and 0.1%, respectively, full details given in Tanaka & McAllen (2005). To identify injection sites, 1% red fluorescent microspheres (FluoSperes, Molecular Probes) was added to the injectate. A glass micropipette (tip o.d. $\sim$50 μm) filled with PGE_2 solution (including fluorescent microspheres) was positioned stereotaxically in the right preoptic area (POA) (0.3–1.0 mm from the midline, between 0.1 mm anterior and 0.3 mm posterior to bregma, and 8.0–9.0 mm below the dural surface). PGE_2 was injected in volumes of 120 nl, at times when both sympathetic nerve activities were low and stable.

Muscimol injection into the medullary raphé. Muscimol (Sigma) was diluted with aCSF, and mixed with 2% green fluorescent microspheres (FluoSperes) to identify injection sites. A glass micropipette filled with 2 mM muscimol was positioned stereotaxically into the rostral medulla (3.0 mm posterior to lambda, 0.0–0.5 mm lateral to midline, and 9.5 mm deep to the dural surface), aimed at the ventral medullary raphé at the level of the caudal part of the facial nucleus (Morrison, 1999; Morrison *et al.* 1999; Ootsuka *et al.* 2004; Ootsuka & McAllen, 2005).

In 8 of 9 rats, including one rat where tail SNA was not recorded, a series of 60 s cooling episodes starting from warm baseline conditions were used to activate both tail SNA and back skin SNA. Muscimol was injected through the micropipette in volumes of 60 nl ($n = 5$) or 120 nl ($n = 3$) over approximately 60 s, 4–5 min after the last cooling episode; the cooling protocol was then continued for two cycles afterwards. In 6 of 9 rats, vehicle (aCSF, 120 nl) was also microinjected into the medullary raphé during a period when tail ($n = 5$) and back skin SNA ($n = 6$) were activated by trunk skin cooling.

At the end of the experiment animals were deeply anaesthetized with pentobarbitone sodium (325 mg, I.V.) and perfused transcardially with saline followed by 4% paraformaldehyde. The brain was removed and placed in the same fixative at least overnight. After cryoprotection with 20% sucrose in phosphate-buffered saline, 40 μm frozen coronal sections were made of the preoptic area and medulla. The locations of microinjection sites were identified by detecting the fluorescent microspheres, using fluorescence microscopy (Axioplan 2 imaging, Carl Zeiss, Germany). Relevant sections were photographed under both light and fluorescence optics using a digital camera (AxioCam HRc, Carl Zeiss). Anatomical detail was revealed by contrast reversal of the light microscopic image in Adobe Photoshop. In each case the centre of the injection was identified and mapped onto sections of the atlas of Paxinos & Watson (1998).

Statistical analysis

The baseline core temperature, skin temperature, blood pressure, heart rate, tail SNA (spikes $10\ s^{-1}$) and back skin SNA (spikes $10\ s^{-1}$) were measured as the average values of these variables over 1 min just before each stimulation.

Temperature thresholds and thermal sensitivities of both tail SNA and back skin SNA were estimated by plotting 10 s spike counts against either skin or core temperature, as previously described (Owens *et al.* 2002). For this purpose, data were selected from sections of the record where the nerve activity in question was driven by only skin or only core temperature, not both (i.e. the other influence was subthreshold, see below). In the case of skin temperature, data were taken from the first skin cooling period which generated $>$ 10% maximal activity in the nerve concerned. In the case of core temperature, data were taken from the rewarming phase following a cooling sequence, after skin temperature had been warmed beyond its threshold yet residual activity, driven by low core temperature, remained. That opportunity did not arise for tail SNA in three animals, whose data were therefore not used for measurements of thermal thresholds and K ratios (see below).

Thresholds were estimated from the intercept of the regression line of the relation between nerve activity and skin or core temperature. The slopes of the regression lines were used to estimate the thermal sensitivities of each nerves to skin cooling (K_{skin}) and core cooling (K_{core}); the ratio of K_{core} to K_{skin} (K ratio: K_{core}/K_{skin}, Owens *et al.* 2002) was calculated for each nerve in each animal. Student's paired t test was used to compare threshold skin and core temperatures between tail and back skin SNA, and to compare, within animals, the difference between the K ratios for back skin and tail SNA.

To analyse the effect of preoptic PGE_2 injections, pre-injection baseline values and peak responses of each variable were averaged over 1 min periods. These were compared, using either Student's paired t test or the Wilcoxon signed-rank test (for non-normally distributed data). The onset of tail and back skin SNA activation was taken as the time when it reached 10% of its subsequent peak firing rate. The time to onset and the durations of tail

SNA and back skin SNA responses were compared using Student's paired *t* test.

To assess the effect of muscimol injection into the medullary raphé on tail SNA and back skin SNA, one-way repeated ANOVA or the Friedman test (for non-normally distributed data), followed by Tukey test, was used to compare nerve firing rate under the following conditions: (1) 1 min average just before muscimol injection; (2) 1 min average 4–5 min after muscimol injection (just before subsequent cooling episodes); and (3) at the nadir of the second subsequent skin cooling episode (1 min average). To assess the effect of vehicle injections, a paired *t* test was used to compare 1 min averages of tail and back skin SNA taken just before, and 5 min after vehicle injection. All values were shown as mean ± S.E.M. and $P < 0.05$ was considered significant.

Signal processing

Cardiac and respiratory rhythmicities in tail and back skin sympathetic activities were analysed by constructing histograms of discriminated activity triggered by the arterial pulse (using 10 ms bins) or lung inflation (100 ms bins). In the case of whole nerve back skin SNA, the threshold for discrimination was set above the noise level measured after hexamethonium. Data were taken from 300 s periods of approximately steady-state activity induced, where appropriate, by cooling. The strength of rhythmicity was measured from the histogram as (maximum − minimum)/maximum in eight successive bins, as described elsewhere (Boczek-Funcke *et al.* 1991; Gilbey & Stein, 1991; Häbler *et al.* 1993), and a threshold value considered to determine the presence of rhythmicity was set at 30%. Student's paired *t* test was used to compare the degree of cardiac rhythmicity of back skin SNA between warm baseline conditions and during cooling.

For spectral analysis, discriminated tail SNA and back skin SNA spikes were converted to waveforms using the sinc function (defined as $(\sin x)/x$) in Spike 2, to reflect the interspike intervals rather than the shape of spikes (Christakos *et al.* 1984; Barman & Gebber, 1997). Converted nerve signals, blood pressure and respiratory pressure were then digitized at 100 Hz, and any DC component was removed from the signal.

To generate autospectra, fast Fourier transformation (FFT) was performed on 122.88 s of data, segmented into 23 half-overlapped blocks of 10.24 s, each of which was transformed by a Hanning window. The FFT size of 1024 points gave a spectral resolution of 0.1 Hz. Autospectra of the 23 segments were averaged and expressed as the percentage of total power between 0 and 15 Hz. Student's paired *t* test was used to compare amplitudes of ∼1 Hz peaks between tail and back skin fibre activity. To reveal linear correlations between signals, coherence spectra were calculated from the same 23 half-overlapped blocks. Partial coherence spectra were also used to observe the relationship between tail and back skin SNA after mathematical removal of the influence of third signal such as cardiac or respiratory cycles (Kocsis, 1994). Coherence at a particular frequency was considered significant ($P < 0.05$) if it exceeded 0.127, which was calculated from the equation given by Rosenberg *et al.* (1989): $1 - P^{1/(L-1)}$, where P is probability and L is the number of segments used to calculate coherence.

Results

Preliminary experiments

To assess the sympathetic supply to back skin (back skin SNA), recordings were made initially from the whole nerve in eight urethane-anaesthetized rats. Starting from warm background conditions, when activity was at its minimum, back skin SNA increased in response to cooling the trunk skin (Fig. 1*A*). This activity was blocked by hexamethonium (Fig. 1*A*, end). Under warm baseline conditions, however, a tonic level of activity remained (compare signal amplitudes at the beginning and end of Fig. 1*A*). That tonic activity showed strong cardiac rhythmicity (93 ± 2%, $n = 8/8$, see Methods), as shown by cardiac cycle-triggered histograms (Fig. 1*B*). This firing pattern is similar to that of vasoconstrictor (MVC) fibres supplying skeletal muscle (Häbler *et al.* 1994; Jänig & Häbler, 2003). On the other hand, the higher amplitude signal which was activated by cooling showed much less cardiac rhythmicity (53 ± 5%, $n = 8$, $P < 0.01$), as shown in Fig. 1*C*. This firing pattern is similar to that demonstrated for cutaneous vasoconstrictor (CVC) fibres supplying hindlimb skin (Häbler *et al.* 1994) or tail (Johnson & Gilbey, 1994; Häbler *et al.* 1999; Owens *et al.* 2002).

To investigate whether the mixed character of whole back skin nerve activity was due to (a) the summed activity of two independent classes of sympathetic fibre, or (b) due to a population of fibres with 'mixed' characteristics, we split these nerves and recorded few-fibre activity in nine rats. For comparison, single fibre ($n = 1$) or few-fibre (2–4 units) activity ($n = 8$) was recorded simultaneously from the tail. The characteristics of tail SNA was similar to that described in previous studies (Johnson & Gilbey, 1994; Häbler *et al.* 1999; Owens *et al.* 2002; Ootsuka & McAllen, 2006): from a silent baseline under warm conditions it was activated by trunk skin and core cooling, and its activity was modulated by the ventilatory cycle. Single unit activity was discriminated from back skin SNA recordings, using spike shape analysis. Units fell into two distinct categories: one type (MVC-type) was tonically active in warm conditions, was not affected by cooling but showed strong cardiac rhythmicity (100% in 5/5 units in 2 rats, Fig. 2). The

second type (CVC-type) was silent under warm conditions but activated by cooling; in most (7/9) preparations, these fibres showed no cardiac rhythmicity (Figs 2 and 3*B*). Both MVC-type and CVC-type fibre activities were abolished by hexamethonium (50 mg kg^{-1}), demonstrating that they were of postganglionic sympathetic origin (not shown). MVC-type units were not analysed further. Few-fibre (2–6 units) preparations containing only CVC-type units were selected for further study, and their activity was compared with simultaneously recorded units supplying the tail.

Figure 3 shows representative extracts of the activity of CVC-type back skin fibres and tail fibres recorded simultaneously during cooling. Cycle-triggered histograms of this cold-evoked activity show that in this case, the back skin CVC-type activity had no obvious cardiac or ventilatory rhythmicity, while the tail fibres showed pronounced cardiac and ventilatory modulation (Fig. 3*B* and *C*). Overall, back skin CVC-type fibres showed cardiac rhythmicity in 2 of 9 rats (50 and 45%) and ventilatory modulation in 1 other rat (48%). Tail fibres, by contrast, showed cardiac modulation in 4 of 9 rats (63 ± 8%) and ventilatory modulation in all 9 animals (68 ± 6%).

Responses to cooling

Figure 4 shows a chart record of the activity of simultaneously recorded tail and back skin CVC-type fibres, displayed as 10 s spike counts from few-fibre preparations. Under warm baseline conditions (skin temperature 39.9 ± 0.2°C, core temperature 38.2 ± 0.2°C, $n = 6$), both tail and back skin CVC-type activities were low or silent. Animals were subjected to a sequence of brief skin cooling episodes by perfusing cold water through the water jacket. Each 30 s cooling episode lowered skin temperature by 1.5–3.5°C, and the sequence of 8–10 cooling episodes caused core temperature to fall to 36.0 ± 0.2°C. As established previously (Owens *et al.* 2002; Ootsuka & McAllen, 2006), components of tail fibre activation were attributable both to the immediate fall in skin temperature and to the delayed fall in core temperature (Fig. 4*A*). The threshold skin temperature for

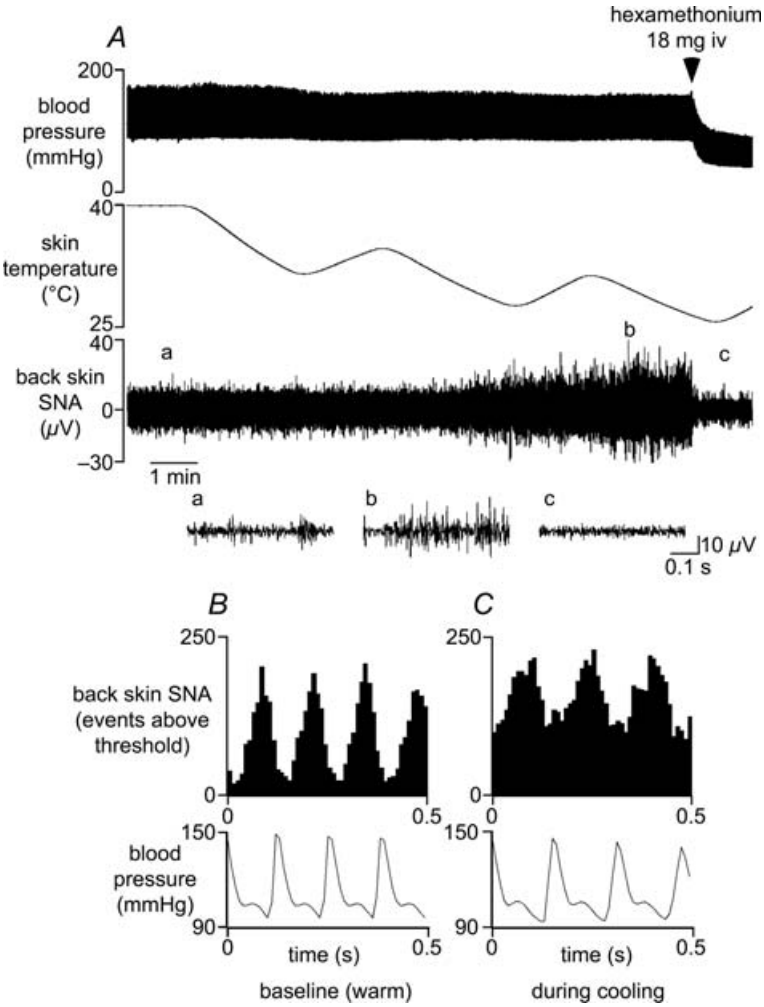

Figure 1. Properties of sympathetic nerve discharge to back skin
A, chart record from a representative experiment showing (from top) blood pressure, skin temperature and sympathetic activity recorded from the central end of a nerve supplying back skin (back skin SNA). Shown below the chart record are 3 expanded records of back skin SNA, taken from times denoted on the lower trace: (a) before skin cooling, (b) during skin cooling and (c) after ganglion blockade with hexamethonium (indicated above upper trace). *B* and *C* show arterial pulse-triggered histograms of the ongoing back skin SNA (counted events above threshold) during warm baseline conditions (*B*) and during skin cooling (*C*) (10 ms bins; 6378 and 9912 events, respectively). Bottom traces show the corresponding mean arterial pressure waveforms.

tail fibre activation was $38.8 \pm 0.4^{\circ}$C and threshold core temperature was $38.1 \pm 0.2^{\circ}$C ($n = 6$).

The threshold skin temperature to activate back skin CVC-type fibres was $36.8 \pm 0.4^{\circ}$C ($n = 6$), significantly lower than that for tail SNA ($P < 0.01$). Moreover, as previously described in the case of fusimotor fibres (Tanaka *et al.* 2006), cooling failed to activate back skin CVC-type fibres at the expected skin temperature (shown by the horizontal dashed line in Fig. 4*A*) if the core temperature was relatively warm (as in the second and third skin cooling episodes). At the end of the cooling sequence, a moderate level of back skin CVC-type activity remained in response to the low core temperature (compared with a strong component of tail fibre activity (Fig. 4*A*)). The core temperature threshold for back skin CVC-type fibres was $36.8 \pm 0.2^{\circ}$C ($n = 6$), significantly lower than the corresponding value for tail SNA ($n = 6$; $P < 0.01$).

The response profiles of tail and back skin CVC-type activity differed in that the incremental activity with each skin cooling episode was large for back skin CVC-type units, but modest for tail units, whose response quickly saturated as core temperature fell (Fig. 4*A*). These differences are shown clearly when responses are plotted against skin or core temperatures (Fig. 4*B–E*). The sensitivities of each nerve to skin and core cooling (K_{skin} and K_{core}) and the K ratio (K_{core}/K_{skin}) were calculated as previously described (Owens *et al.* 2002). In paired comparisons, the K ratio was always lower for back skin CVC-type fibres than that for tail SNA (4.0 ± 1.1 *versus* 21.6 ± 5.7; $P < 0.05$, $n = 6$).

Responses to PGE_2 in the preoptic area

Unilateral injections of 30 ng PGE_2 into the preoptic area (POA) of nine rats caused core (rectal) temperature to increase, starting 1.6 ± 0.3 min after the injection and reaching 0.9–1.8°C (mean $1.3 \pm 0.1^{\circ}$C) above resting levels. Blood pressure also increased from 91 ± 4 to 107 ± 4 mmHg ($P < 0.01$; $n = 9$) and heart rate from 390 ± 15 to 468 ± 16 beats min^{-1} ($P < 0.01$; $n = 9$). There was also a rise in expired CO_2 levels and an increased excursion of the ventilatory pressure signal, indicating active breathing against the ventilatory pump (not shown).

In all nine rats tested, PGE_2 injections significantly increased tail SNA (from 1 ± 1 to 67 ± 11 spikes (10 s)$^{-1}$, $n = 9$, $P < 0.01$)(Fig. 5). Tail SNA began to increase

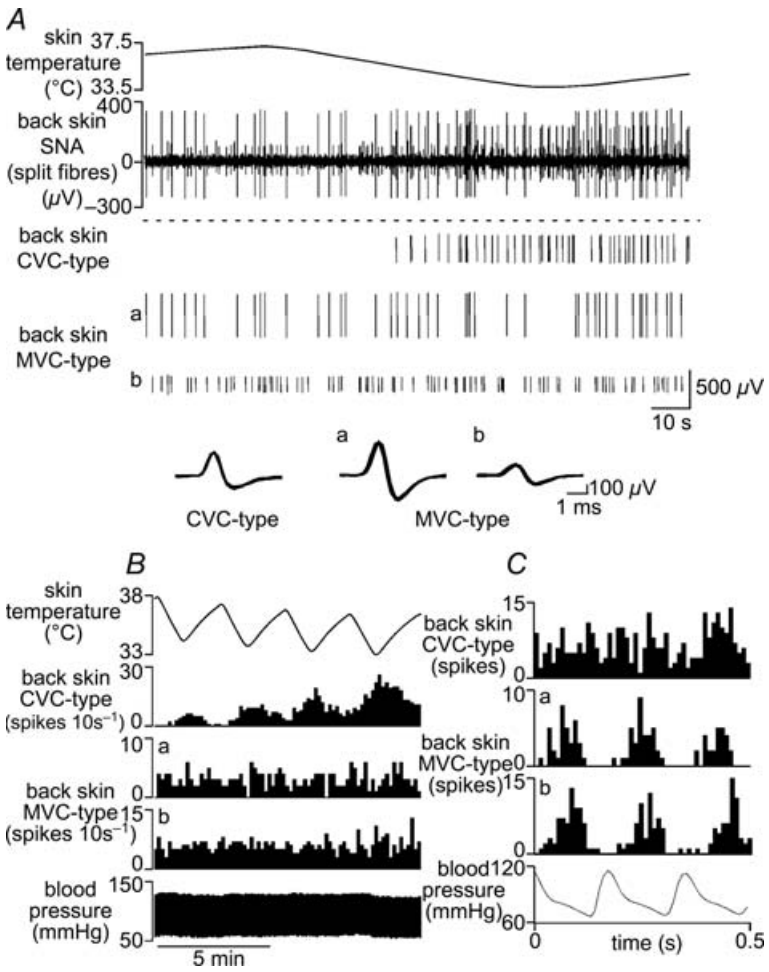

Figure 2. Firing patterns of back skin MVC-type and CVC-type fibres
A, traces from top show: skin temperature; few-fibre activity in a filament split from the nerve to back skin; identified single unit spikes extracted from the neurogram (1 CVC-type and 2 MVC-type fibres, denoted *a* and *b*). Their individual waveforms (superimposed spikes on expanded timescale) are shown below. *B*, chart record showing skin temperature (top trace), blood pressure (bottom trace) and the responses of the same three single units (as indicated) to four successive episodes of skin cooling. *C*, arterial pulse-triggered histograms of the ongoing activity (during cooling) of the same three single units (10 ms bins, from top 350, 96 and 185 counted spikes), shown above the corresponding arterial pressure waveform.

1.3 ± 0.3 min after the PGE_2 injection, and the response lasted 54.8 ± 4.9 min. Back skin CVC-type fibres were activated by this stimulus in seven of the same nine rats; in those seven rats, activity increased from 0 to 39 ± 18 spikes $(10\ s)^{-1}$ ($n = 7$, $P < 0.05$). In the two rats where back skin CVC-type fibres failed to respond to PGE_2, it responded normally to cooling before and afterwards. When responding to PGE_2, back skin CVC-type fibres were always activated later than tail fibres (latency 6.2 ± 1.3 min *versus* 1.0 ± 0.1 min, respectively; $P < 0.01$, $n = 7$) and always stopped firing earlier (mean duration 16.6 ± 3.9 min, range 2.5–34 min, compared with 54.8 ± 4.9 min, range 36–71 min for tail fibres, $P < 0.01$, $n = 7$).

Effect of neuronal inhibition in the medullary raphé

Inhibition of rostal medullary raphé neurons has been shown to inhibit vasoconstrictor fibres supplying the rat's tail and rabbit's ear and to block their responses to cold (Ootsuka *et al.* 2004; Ootsuka & McAllen, 2005). In eight rats, including one where tail SNA was not recorded, we tested whether this also applied to back skin CVC-type fibres. Figure 6 shows a representative record. Sequential (3–7) 60 s cooling episodes lowered skin temperature from 40.2 ± 0.3°C to 32.0 ± 0.4°C and led to a delayed fall in core temperature from 38.3 ± 0.2°C to 36.2 ± 0.4°C ($n = 8$): both tail and back skin CVC-type fibres were strongly activated (Fig. 6*A* and Table 1). Muscimol (120–240 pmol in 60–120 nl) microinjected into the medullary raphé significantly inhibited tail fibre activity ($P < 0.05$, $n = 7$), and silenced back skin CVC-type fibres ($P < 0.05$, $n = 8$; Fig. 6*A*, right and Table 1). Tail fibre activity was silenced in 2 of 2 rats after they received 240 pmol muscimol in the medullary raphé, but a low level of tonic tail fibre activity remained after muscimol injection in 5 of 5 rats which received 120 pmol (e.g. Fig. 6*A*, right). Blood pressure fell slightly (from 80 ± 2 to 73 ± 2 mmHg, $n = 8$). After raphé-muscimol injection, the skin cooling sequence was repeated for two further cycles (Fig. 6*A*, right), which lowered skin temperature from 38.2 ± 0.3°C to 32.2 ± 0.4°C and core temperature from 35.9 ± 0.4°C to 35.6 ± 0.4°C ($n = 8$), but failed to increase tail or back skin CVC-type fibre activity (Fig. 6*A*, right and Table 1).

Previous microinjection of vehicle (120 nl) into the medullary raphé had no significant effect on tail ($n = 5$) or back skin CVC-type activity ($n = 6$). The non-significant reduction in back skin CVC-type activity after vehicle injection (Table 1) is attributable to falling activity during rewarming (compare responses to the three cooling episodes in Fig. 6*A*). Post mortem reconstruction of the sites of muscimol injections confirmed that all were positioned close to the ventral medullary raphé, level with the caudal part of the facial nucleus (Fig. 6*B*).

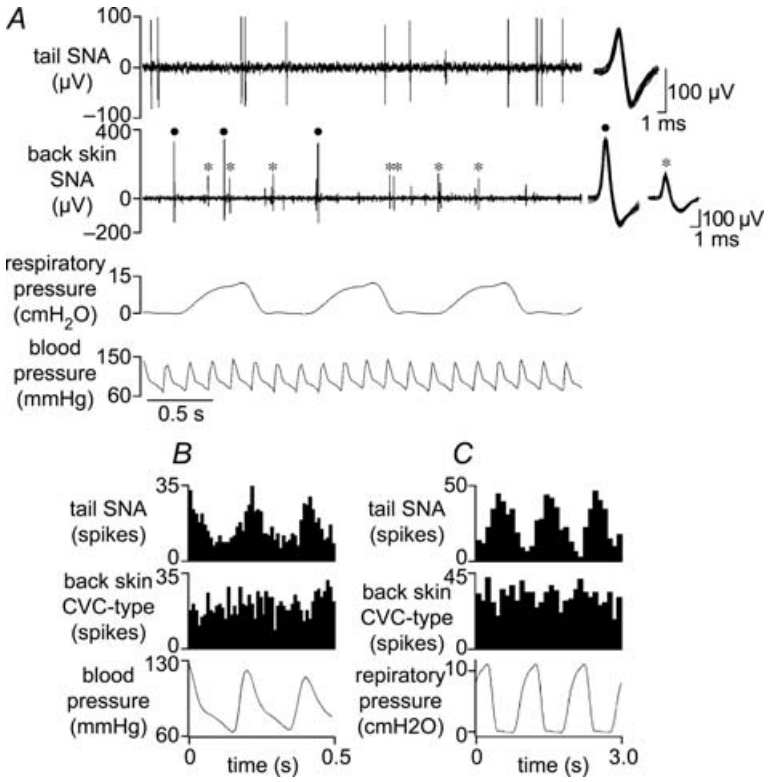

Figure 3. Simultaneous recording of tail sympathetic activity and back skin CVC-type fibre activity
A, chart record showing (from top): sympathetic unit activity recorded from a filament in the lateral collector nerve of the tail (tail SNA), sympathetic activity in a filament split from the nerve to back skin (back skin SNA), respiratory pressure and blood pressure. Filled dots and asterisks in the second trace (back skin SNA) indicate two discriminated single CVC-type units. Superimposed spike shapes of each discriminated single unit are shown at the end of their respective traces. *B* and *C* show arterial pulse-triggered (*B*) and respiratory pressure-triggered (*C*) histograms of tail SNA and back skin CVC-type fibre activity during cooling (bin size 10 ms in *B* and 100 ms in *C*; 949 tail SNA spikes and 1237 back skin CVC-type spikes counted in both *B* and *C*).

Spectral analysis

Autospectra and coherence spectra were constructed from sections of record when both tail and back skin CVC-type fibres were in a stable, activated state (during the late phase of a cooling sequence and after PGE_2 injection in the POA) in seven rats. Figures 7 and 8 show representative examples taken from one animal. Figure 7*A* and *B* show tail and back skin CVC-type autospectra (few-fibre preparation) during cooling, while Fig. 8*A* and *B* show the corresponding autospectra after PGE_2 injection in the same animal. In both conditions, autospectra of tail SNA showed a sharp peak at 1 Hz, corresponding to the ventilatory frequency (Chang *et al.* 2000; Ootsuka & McAllen, 2006), and there was significant coherence between tail SNA and respiratory pressure at 1 Hz in all animals (0.59 ± 0.07 during cooling, 0.81 ± 0.07 after PGE_2 injection, $n = 7$) (Figs 7*F* and 8*F*). Autospectra of back skin CVC-type activity showed a less sharp peak around 1 Hz in 5 of 7 rats during cooling and in 4 of 7 rats after PGE_2 injection (Figs 7*B* and 8*B*), and that peak often did not coincide with the ventilatory frequency. Its amplitude was significantly smaller than the 1 Hz peak in the tail fibre autospectum ($0.9 \pm 0.1\%$ *versus* $2.4 \pm 0.3\%$ during cooling, $1.0 \pm 0.1\%$ *versus* $6.6 \pm 1.7\%$ after PGE_2 injection, $P < 0.05$). There was no significant coherence between back skin CVC-type fibre activity and respiratory pressure at 1 Hz during cooling (0 of 7 rats, Fig. 7*H*), but significant coherence was present in 4 of 7 rats after PGE_2 injection (0.37 ± 0.09, $n = 4$) (Fig. 8*H*).

Coherence analysis was also used to test whether common rhythmic inputs influenced the activity of the two nerves. There was no significant coherence between tail and back skin activity during cooling (Fig. 7*I*). After PGE_2 injection, significant coherence was present at ~1 Hz in 4 of 7 rats (coherence value 0.27 ± 0.06, $n = 4$, Fig. 8*I*). Partial coherence (Kocsis, 1994) was used to test whether

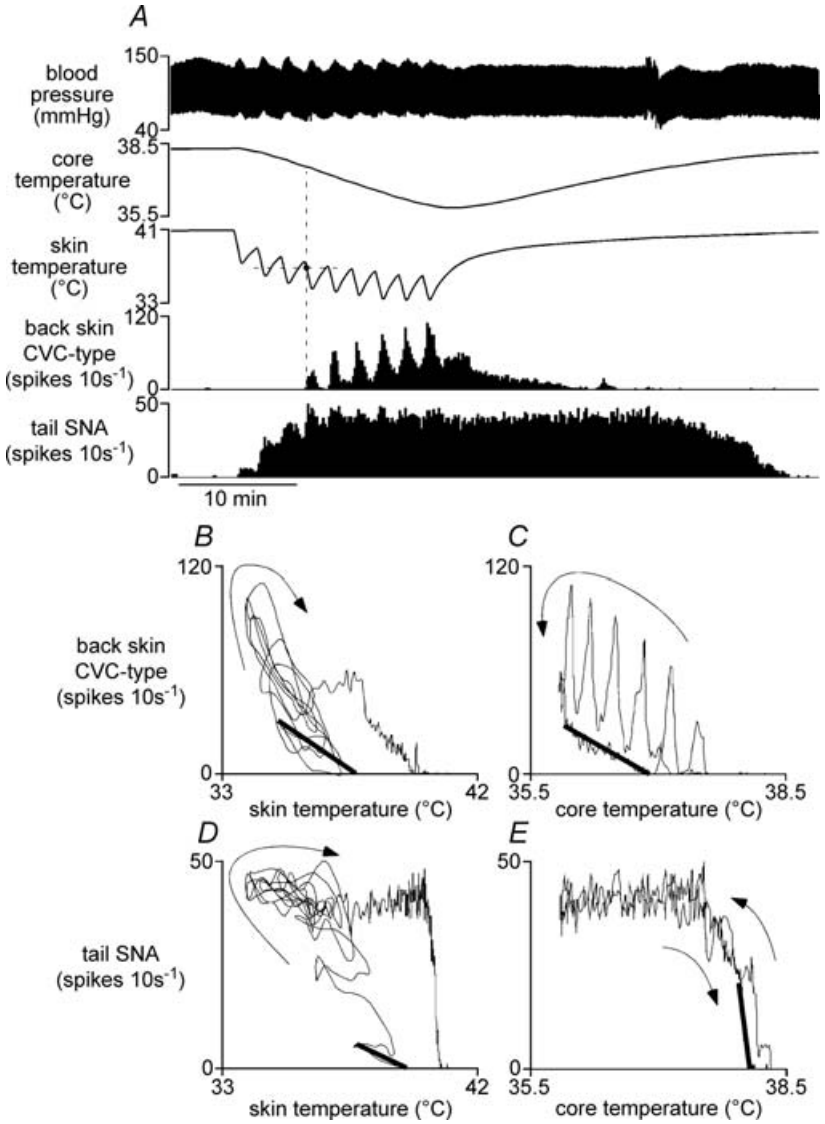

Figure 4. Responses of tail and back skin CVC-type fibres to skin cooling
A, representative chart record showing responses to repeated skin cooling while core temperature was allowed to fall. Traces from top show blood pressure, core (rectal) temperature, skin temperature and few-fibre activities (10 s counts) recorded from back skin CVC-type and tail fibres. Note that when the expected threshold (horizontal dashed line) was crossed during the second and third skin cooling periods, there was no activation of back skin CVC-type fibres. Data from *A* are replotted in *B* and *C* to show back skin CVC-type fibre activity *versus* skin temperature (*B*) and *versus* core temperature (*C*). *D* and *E* show corresponding plots of tail SNA *versus* skin and core temperatures. Linear regression lines (thick lines) were calculated from appropriate sections of the record to estimate threshold skin temperature and K_{skin} (*B* and *D*), and threshold core temperature and K_{core} (*C* and *E*) for each nerve (see Methods). Arrows indicate the time sequence of plotted points.

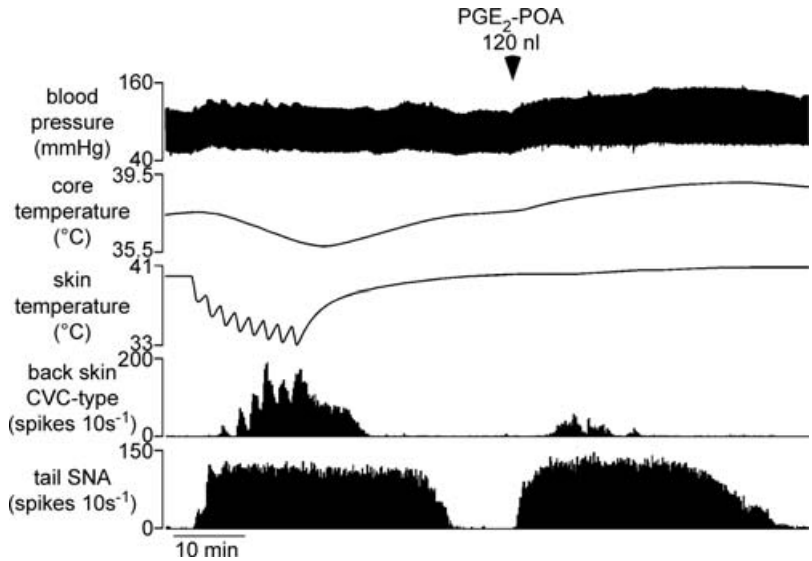

Figure 5. Responses of tail and back skin CVC-type fibres to prostaglandin E_2 (PGE_2) injection into the preoptic area
Traces from top show blood pressure, core (rectal) temperature, skin temperature and few-fibre activity (10 s counts) of back skin CVC-type and tail fibres. After recovery from a standard cooling sequence (left of trace), PGE_2 (30 ng in 120 nl) was injected into the preoptic area (POA) at the time indicated.

that 1 Hz coherence between the two nerves after PGE_2 injection was attributable to common modulation by the ventilatory cycle (Ootsuka & McAllen, 2006). After partialization with respect to the respiratory pressure signal, no significant coherence peak remained (peak coherence at 1 Hz from 0.27 ± 0.06 to 0.05 ± 0.02; $n = 4$, Fig. 8*J*).

Discussion

This study documents, for the first time, the comparative behaviour of the vasomotor supplies to proximal hairy skin (back) and hairless skin (tail) in the context of thermoregulation. Quantitative differences may reasonably have been expected, but the results indicate that these

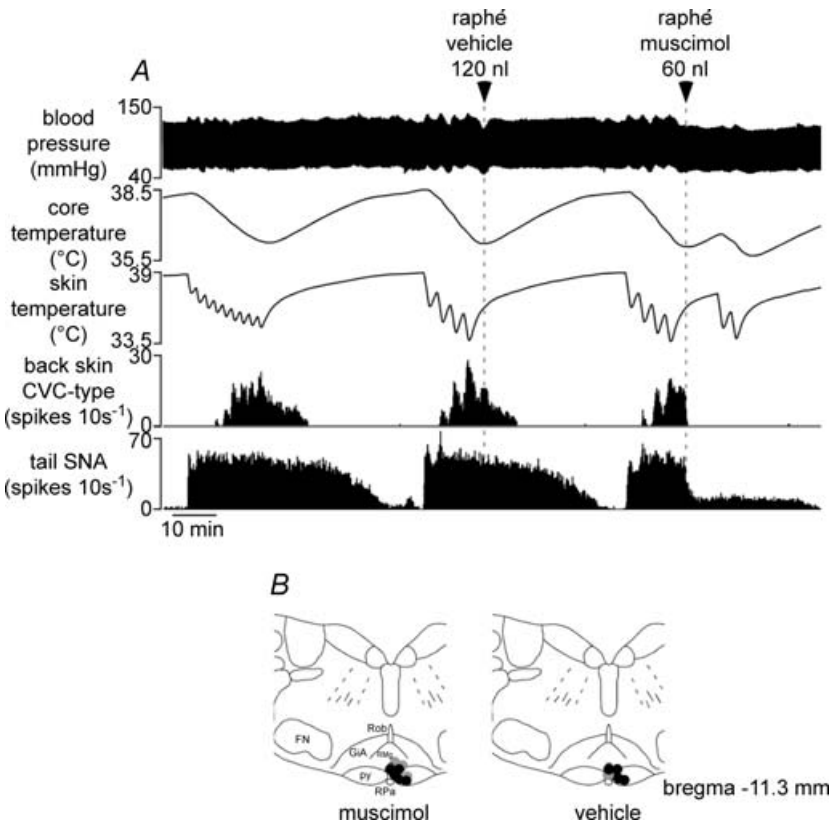

Figure 6. Effect of neuronal inhibition in the medullary raphé on tail and back skin CVC-type fibre responses to skin cooling
A, traces from top show blood pressure, core (rectal) temperature, skin temperature and few-unit activity (10 s spike counts) recorded from back skin CVC-type and tail fibres. Vehicle (aCSF 120 nl, middle) and muscimol (120 pmol in 60 nl, right) were injected, as indicated by arrowheads and dashed lines, at times when tail and back skin CVC-type fibres were activated by cooling. *B*, muscimol and vehicle injection sites plotted onto a standard section, drawn with reference to the atlas of Paxinos & Watson (1998) at the level indicated. Grey circles indicate sites where either muscimol or vehicle was injected alone. Black circles indicate sites where both muscimol and vehicle were injected in the same animal. Abbreviations: GiA, gigantocellular reticular nucleus pars alpha; FN, facial nucleus; py, pyramidal tract; RMg, raphé magnus nucleus; ROb, raphé obscurus nucleus; RPa, raphé pallidus nucleus.

Table 1. Changes in nerve activity after raphé muscimol or vehicle injection

Raphé-muscimol		Before injection	After injection	Subsequent cooling
Tail SNA	$n = 7$	52 ± 10	$19 \pm 6^*$	$18 \pm 6^*$
Back skin CVC-type	$n = 8$	39 ± 22	$1 \pm 0.4^*$	$8 \pm 8^*$
Raphé-vehicle		**Before injection**	**After injection**	
Tail SNA	$n = 5$	52 ± 13	48 ± 12	
Back skin CVC-type	$n = 6$	42 ± 20	23 ± 10	

Values shown are 1 min means of activity (10 s spike counts) ± S.E.M. Columns show values just before raphé injection, 4–5 min after the injection (just before subsequent cooling), and at the nadir of the second subsequent cooling episode (after muscimol injection). *Significant differences ($P < 0.05$) from activity before the injection. After muscimol injection, subsequent cooling caused no further significant change. Raphé-vehicle injections also caused no significant change.

two sympathetic outflows may be driven by entirely independent neural systems. Tail and back skin CVC-type fibres differed in their thermal thresholds, their thermal sensitivities, their relative responsiveness to skin and core temperatures and to experimental fever; their ongoing activity showed different patterns of rhythmicity, and spectral analysis confirmed their lack of common drive patterns. Nevertheless, the cold-induced activity in central drive pathways to both tail and back skin vessels depends on critical synaptic relays in the medullary raphé.

One novel finding of this study was that two sympathetic fibre types are active in the nerve to back skin: not only CVC-type fibres but also MVC-type fibres, which presumably supply blood vessels in the panniculus carnosus immediately beneath the skin. We consider it unlikely that any pilomotor fibres were active under our experimental conditions: no visible movement occurred in the unshaved hair during cooling (authors' unpublished observations), and extreme measures such as 3–4 min of asphyxia are necessary to induce pilomotor activity in anaesthetized animals (Grosse & Jänig, 1976).

Thermoregulatory responses of the CVC supply to hairy and hairless skin have previously been investigated in the hindlimb of the cat. These were found to be inhibited by warming the hypothalamus or spinal cord, but to respond only weakly to cooling of those areas (Grewe *et al.* 1995). How the vasomotor supply to proximal hairy skin responds to cutaneous (ambient) temperature does not appear to have been studied previously in laboratory animals.

The activity patterns of CVC fibres supplying the hairy skin of the hindlimb have been previously studied in rats. The cardiac rhythmicity of these fibres has been reported as generally weak (Häbler *et al.* 1994), but their propensity to be modulated by the respiratory cycle (both by central respiratory drive and by lung inflation) is strong (Häbler *et al.* 1993). This is also the case for tail fibres (Johnson & Gilbey, 1994; Häbler *et al.* 1999). A third rhythm found in the CVC supply to the skin of the foot and tail – the 'T-rhythm' – may be also entrained by the ventilatory and central respiratory cycles (Chang *et al.* 2000).

In the present study we made no attempt to dissociate ventilatory, central respiratory or T-rhythm components in nerve discharges. We may infer, however, that ventilation-related rhythms are not prominent in back skin CVC-type activity, at least during cooling. In some rats, however, coherence between back skin CVC-type activity and ventilatory pressure appeared after PGE_2 injection into the POA. One possible reason for this could be that a raised central respiratory drive during hyperthermia (Boden *et al.* 2000; Häbler *et al.* 2000), with perhaps an additional component due to the febrile stimulus, exceeded a threshold necessary for an effect on back skin CVC-type activity. Even under febrile conditions, however, ventilatory modulation of back skin CVC-type was present in only 4 of 7 rats, and was always weaker than for tail fibres.

Another difference between tail and back skin CVC-type fibres was that PGE_2 injections into the POA did not always activate the latter, even though all injections were made into effective sites, as judged by tail fibre activation and a rise in rectal temperature. This may be because the preoptic neurons driving back skin CVC-type fibres are less sensitive to febrile stimuli than the preoptic neurons driving tail fibres, as is evidently the case for thermal stimuli. It could also be that their less consistent and less prolonged activation by PGE_2 compared with tail fibres is because back skin CVC-type fibres were further away from their thermal thresholds (see Fig. 5), and thus less excitable at the time.

The present findings on the behaviour of back skin CVC-type fibres may now be compared with other cold-activated neural responses. In this laboratory we have examined four such responses in rats under similar experimental conditions with a similar protocol: tail fibres (Owens *et al.* 2002; Ootsuka & McAllen, 2006; this study), back skin CVC-type fibres (this study), sympathetic fibres innervating interscapular brown adipose tissues (BAT) (Ootsuka & McAllen, 2006) and fusimotor fibres (Tanaka *et al.* 2006). We can therefore report with confidence that each outflow has its characteristic thermal thresholds and its characteristic relative responsiveness

to core *versus* skin temperature changes (expressed by the K ratio: K_{core}/K_{skin}). Tail fibres always showed a high K ratio, reflecting their dominant control by body core temperature. Fusimotor neurons showed no sensitivity to core cooling (Tanaka *et al.* 2006); their K ratios would consequently have been zero. In contrast, BAT and back skin CVC-type fibres showed intermediate K ratio values (Ootsuka & McAllen, 2006; this study), indicating moderate sensitivity to both skin and core temperatures. We cannot discount the possibility that the method of skin

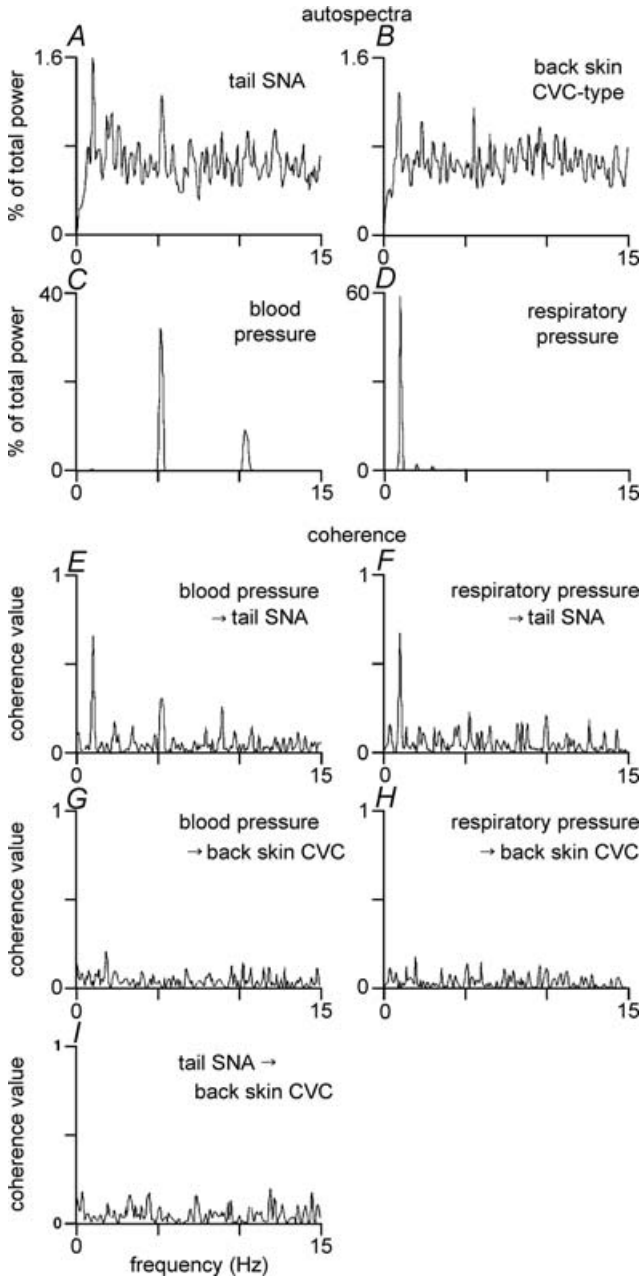

Figure 7. Spectral analysis of tail SNA and back skin CVC-type fibre activity during skin cooling
Examples for illustration are taken from a single representative experiment. Panels *A–D* show autospectra (% of total power between 0 and 15 Hz) of tail SNA (few-fibres, *A*), back skin CVC-type fibre activity (few-fibres, *B*), blood pressure (*C*) and respiratory pressure (*D*). Panels *E–H* show coherence spectra of tail SNA with respect to blood pressure (*E*) and respiratory pressure (*F*), and coherence spectra of back skin CVC-type fibre activity with respect to blood pressure (*G*) and respiratory pressure (*H*). The coherence spectrum between tail SNA and back skin CVC-type fibre activity is shown in *I*: note the absence of any clear peak.

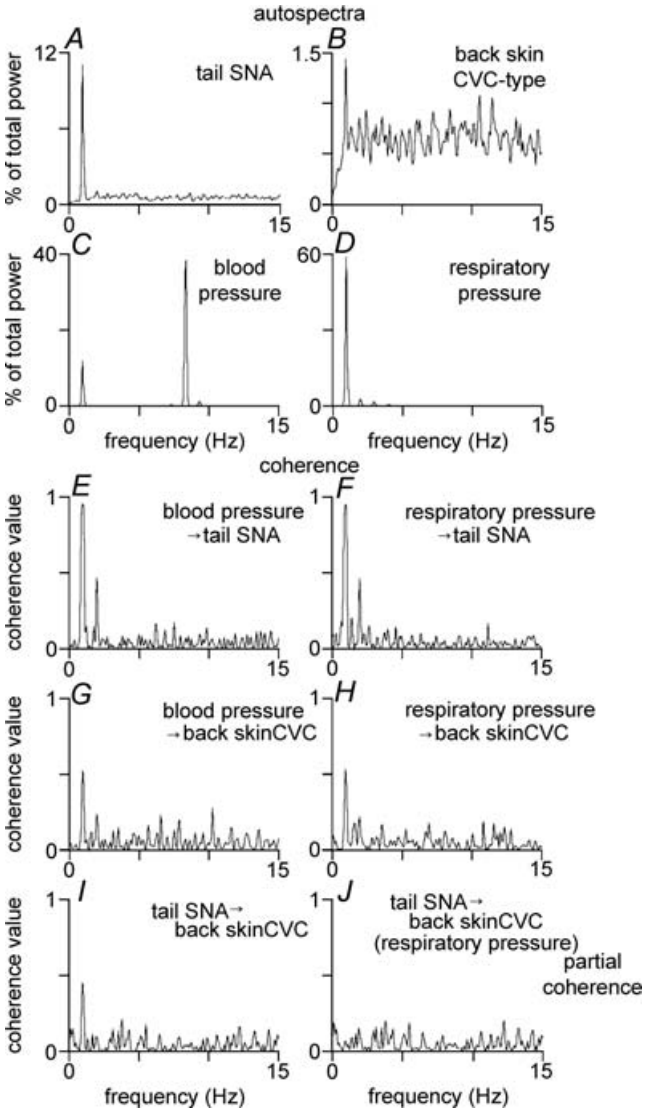

Figure 8. Spectral analysis of tail SNA and back skin CVC-type fibre activity after PGE_2 injection into the preoptic area
Examples for illustration are taken from the same experiment as in Fig. 7. Panels *A–D* show autospectra (% of total power between 0 and 15 Hz) of tail SNA (few-fibres, *A*), back skin CVC-type fibre activity (few-fibres, *B*), blood pressure (*C*) and respiratory pressure (*D*). Panels *E–H* show coherence spectra of tail SNA with respect to blood pressure (*E*) and respiratory pressure (*F*), and coherence spectra of back skin CVC-type fibre activity with respect to blood pressure (*G*) and respiratory pressure (*H*). Panels *I* and *J* show coherence spectra between tail SNA and back skin CVC-type fibre activity: note the clear peak around 1 Hz in panel *I*, which disappeared after partialization to remove the common influence on the two signals related to respiratory pressure (panel *J*).

cooling (a jacket around the animal's trunk) could have activated reflexes with 'local sign', having a stronger effect on thoracic (e.g. back skin CVC-type or BAT) than lumbar (e.g. tail) sympathetic outflows: these arguments do not apply to the actions of core temperature or experimental fever, however. Moreover, we have also found from spectral analysis of simultaneous neural recordings from tail fibres with BAT fibres (Ootsuka & McAllen, 2006), and from tail fibres with back skin CVC-type fibres (this study), that their central drive pathways show quite distinct activity patterns. We conclude that these different neural outflows, though all activated by cooling, are each driven by independent central neural pathways.

Functional and anatomical evidence indicates that medullary raphé neurons, presumably premotor neurons (Nakamura *et al.* 2004), mediate several cold-defense responses, including cutaneous vasoconstriction of rat's tail and rabbit's ear (Ootsuka *et al.* 2004), thermogenesis by interscapular BAT (Morrison, 1999; Morrison *et al.* 1999), fusimotor neuron activation (Tanaka *et al.* 2006) as well as visceromotor and secretor responses in the gastrointestinal tract (Bonaz & Taché, 1994). To this list, we may now add the vasomotor supply to hairy skin.

What might be the significance for thermoregulatory function of these differences in vasomotor control of hairy and hairless skin? Under natural conditions outside the rat's nest, skin temperature would almost always be below the thresholds necessary to keep both tail and back skin CVC-type fibres tonically active. Our data indicate that when the animal enters a warm ambient temperature, hairy skin would vasodilate before the tail. This system would have limited capacity to dissipate heat, however, because its blood flow increases only by about 50% in the warm (Rendell *et al.* 1998) and because of the insulating effect of hair. It therefore represents a fine control mechanism for heat loss. By contrast, hairless areas such as the tail and plantar surfaces can dissipate heat much more effectively when their vasoconstrictor tone is removed (O'Leary *et al.* 1985; Gordon, 1990), due to good surface conduction and blood flow increases of up to 400% (Rendell *et al.* 1998). Our data indicate that this would be brought into play only after further rises in ambient or core temperatures.

References

Barman SM & Gebber GL (1997). Subgroups of rostral ventrolateral medullary and caudal medullary raphe neurons based on patterns of relationship to sympathetic nerve discharge and axonal projections. *J Neurophysiol* **77**, 65–75.

Boczek-Funcke A, Häbler HJ, Jänig W & Michaelis M (1991). Rapid phasic baroreceptor inhibition of the activity in sympathetic preganglionic neurones does not change throughout the respiratory cycle. *J Auton Nerv Syst* **34**, 185–194.

Boden AG, Harris MC & Parkes MJ (2000). A respiratory drive in addition to the increase in CO_2 production at raised body temperature in rats. *Exp Physiol* **85**, 309–319.

Bonaz B & Taché Y (1994). Induction of Fos immunoreactivity in the rat brain after cold-restraint induced gastric lesions and fecal excretion. *Brain Res* **652**, 56–64.

Chang H-S, Staras K & Gilbey MP (2000). Multiple oscillators provide metastability in rhythm generation. *J Neurosci* **20**, 5135–5143.

Christakos CN, Rost I & Windhorst U (1984). The use of frequency domain techniques in the study of signal transmission in skeletal muscle. *Pflugers Archl* **400**, 100–105.

Gilbey MP & Stein RD (1991). Characteristics of sympathetic preganglionic neurones in the lumbar spinal cord of the cat. *J Physiol* **432**, 427–443.

Gordon CJ (1990). Thermal biology of the laboratory rat. *Physiol Behav* **47**, 963–991.

Grewe W, Jänig W & Kümmel H (1995). Effects of hypothalamic thermal stimuli on sympathetic neurones innervating skin and skeletal muscle of the cat hindlimb. *J Physiol* **488**, 139–152.

Grosse M & Jänig W (1976). Vasoconstrictor and pilomotor fibres in skin nerves to the cat's tail. *Pflugers Arch* **361**, 221–229.

Häbler H-J, Bartsch T & Jänig W (1999). Rhythmicity in single fiber postganglionic activity supplying the rat tail. *J Neurophysiol* **81**, 2026–2036.

Häbler H-J, Bartsch T & Jänig W (2000). Respiratory rhythmicity in the activity of postganglionic neurones supplying the rat tail during hyperthermia. *Auton Neurosci* **83**, 75–80.

Häbler H-J, Jänig W, Krummel M & Peters OA (1993). Respiratory modulation of the activity in postganglionic neurons supplying skeletal muscle and skin of the rat hindlimb. *J Neurophysiol* **70**, 920–930.

Häbler H-J, Jänig W, Krummel M & Peters OA (1994). Reflex patterns in postganglionic neurons supplying skin and skeletal muscle of the rat hindlimb. *J Neurophysiol* **72**, 2222–2236.

Jänig W & Häbler H-J (2003). Neurophysiological analysis of target-related sympathetic pathways – from animal to human: similarities and differences. *Acta Physiol Scand* **177**, 255–274.

Johnson CD & Gilbey MP (1994). Sympathetic activity recorded from the rat caudal ventral artery *in vivo*. *J Physiol* **476**, 437–442.

Key BJ & Wigfield CC (1994). The influence of the vantrolateral medulla on thermoregulatory circulation in the rat. *J Auton Nerv Syst* **48**, 79–89.

Kocsis B (1994). Basis for differential coupling between rhythmic discharges of sympathetic efferent nerves. *Am J Physiol Regul Integr Comp Physiol* **267**, R1008–R1019.

Morrison SF (1999). RVLM and raphe differentially regulate sympathetic outflows to splanchnic and brown adipose tissue. *Am J Physiol Regul Integr Comp Physiol* **276**, R962–R973.

Morrison SF, Sved AF & Passerin AM (1999). GABA-mediated inhibition of raphe pallidus neurons regulates sympathetic outflow to brown adipose tissue. *Am J Physiol Regul Integr Comp Physiol* **276**, R290–R297.

Nakamura K, Matsumura K, Hübschle T, Nakamura Y, Hioki H, Fujiyama F, Boldogköi Z, König M, Thiel HJ, Gerstberger R, Kobayashi S & Kaneko T (2004). Identification of sympathetic premotor neurons in medullary raphe regions mediating fever and other thermoregulatory functions. *J Neurosci* **24**, 5370–5380.

O'Leary DS, Johnson JM & Taylor WF (1985). Mode of neural control mediating rat tail vasodilation during heating. *J Appl Physiol* **59**, 1533–1538.

Ootsuka Y, Blessing WW & McAllen RM (2004). Inhibition of rostral medullary raphé neurons prevent cold-induced activity in sympathetic nerves to rat tail and rabbit ear arteries. *Neurosci Lett* **357**, 58–62.

Ootsuka Y & McAllen RM (2005). Interactive drives from two brain stem premotor nuclei are essential to support rat tail sympathetic activity. *Am J Physiol Regul Integr Comp Physiol* **289**, R1107–R1115.

Ootsuka Y & McAllen RM (2006). Comparison between two rat sympathetic pathways activated in cold-defense. *Am J Physiol Regul Integr Comp Physiol* **291**, R589–R595.

Owens NC, Ootsuka Y, Kanosue K & McAllen RM (2002). Thermoregulatory control of sympathetic fibres supplying the rat's tail. *J Physiol* **543**, 849–858.

Paxinos G & Watson C (1998). *The Rat Brain in Stereotaxic Coordinates*, 4th edn. Academic Press, San Diego.

Rathner JA & McAllen RM (1999). Differential control of sympathetic drive to the rat tail artery and kidney by medullary premotor cell groups. *Brain Res* **834**, 196–199.

Rendell MS, Finnegan MF, Healy JC, Lind A, Milliken BK, Finney DE & Bonner RF (1998). The relationship of laser-Doppler skin blood flow measurements to the cutaneous microvascular anatomy. *Microvasc Res* **55**, 3–13.

Rosenberg JR, Amjad AM, Breeze P, Brillinger DR & Halliday DM (1989). The Fourier approach to the identification of functional coupling between neuronal spike trains. *Prog Biophys Mol Biol* **53**, 1–31.

Smith JE & Gilbey MP (2000). Coherent rhythmic discharges in sympathetic nerves supplying thermoregulatory circulations in the rat. *J Physiol* **523**, 449–457.

Tanaka M & McAllen RM (2005). A subsidiary fever center in the medullary raphé? *Am J Physiol Regul Integr Comp Physiol* **289**, R1592–R1598.

Tanaka M, Nagashima K, McAllen RM & Kanosue K (2002). Role of the medullary raphé in thermoregulatory vasomotor control in rats. *J Physiol* **540**, 657–664.

Tanaka M, Owens NC, Nagashima K, Kanosue K & McAllen RM (2006). Reflex activation of rat fusimotor neurons by body surface cooling, and its dependence on the medullary raphé. *J Physiol* **572**, 569–583.

Vianna DML & Carrive P (2005). Changes in cutaneous and body temperature during and after conditioned fear to context in the rat. *Eur J Neurosci* **21**, 2505–2512.

Zhang YH, Hosono T, Yanase-Fujiwara M, Chen XM & Kanosue K (1997). Effect of midbrain stimulations on thermoregulatory vasomotor responses in rats. *J Physiol* **503**, 177–186.

Zhang YH, Yanase-Fujiwara M, Hosono T & Kanosue K (1995). Warm and cold signals from the preoptic area: which contribute more to the control of shivering in rats? *J Physiol* **485**, 195–202.

Acknowledgements

We are most grateful to David Trevaks for his expert help with technical and computing aspects of this study. We also thank the National Health and Medical Research Council of Australia for supporting this study.